

CHAPTER III

MATHEMATICAL MODELLING

This chapter describes the model geometry, model assumption, model formulation which performs the relationship between transient mass transport and Darcy's law and model algorithm in finite difference and finite element methods.

3.1 Model Description

Naturally, shapes of petroleum reservoirs have different geometries. For example, anticline shape has been found where the impermeable rock traps the natural gas under the ground, like an umbrella. Natural gas can be recovered by drilling a well through the impermeable rock. Gas in these reservoirs is typically under extremely high pressure, thereby releasing from the reservoir itself.

In this work, the reservoir model initially assumed the petroleum reservoir as a simple rectangular shape. The model was used to investigate the reservoir behaviors such as pressure distribution, wellbore pressure, bottom well pressure and production time after gas withdrawal or injection. Afterwards, the interior islands and curved edge were added into the regular shape to simulate more realistic the reservoir behaviors.

The geometries of reservoir are illustrated in Figures 3.1(a), (b) and (c). The white and gray regions represent the permeable and impermeable rock, respectively. The reservoir was surrounded by impermeable rock or water that no mass transfer along these boundaries. Figure 3.1(c) illustrates the actual reservoir geometry which contains 12 withdrawal wells (white dots) and is surrounded by impermeable rock. The size of this reservoir performs in SI unit.

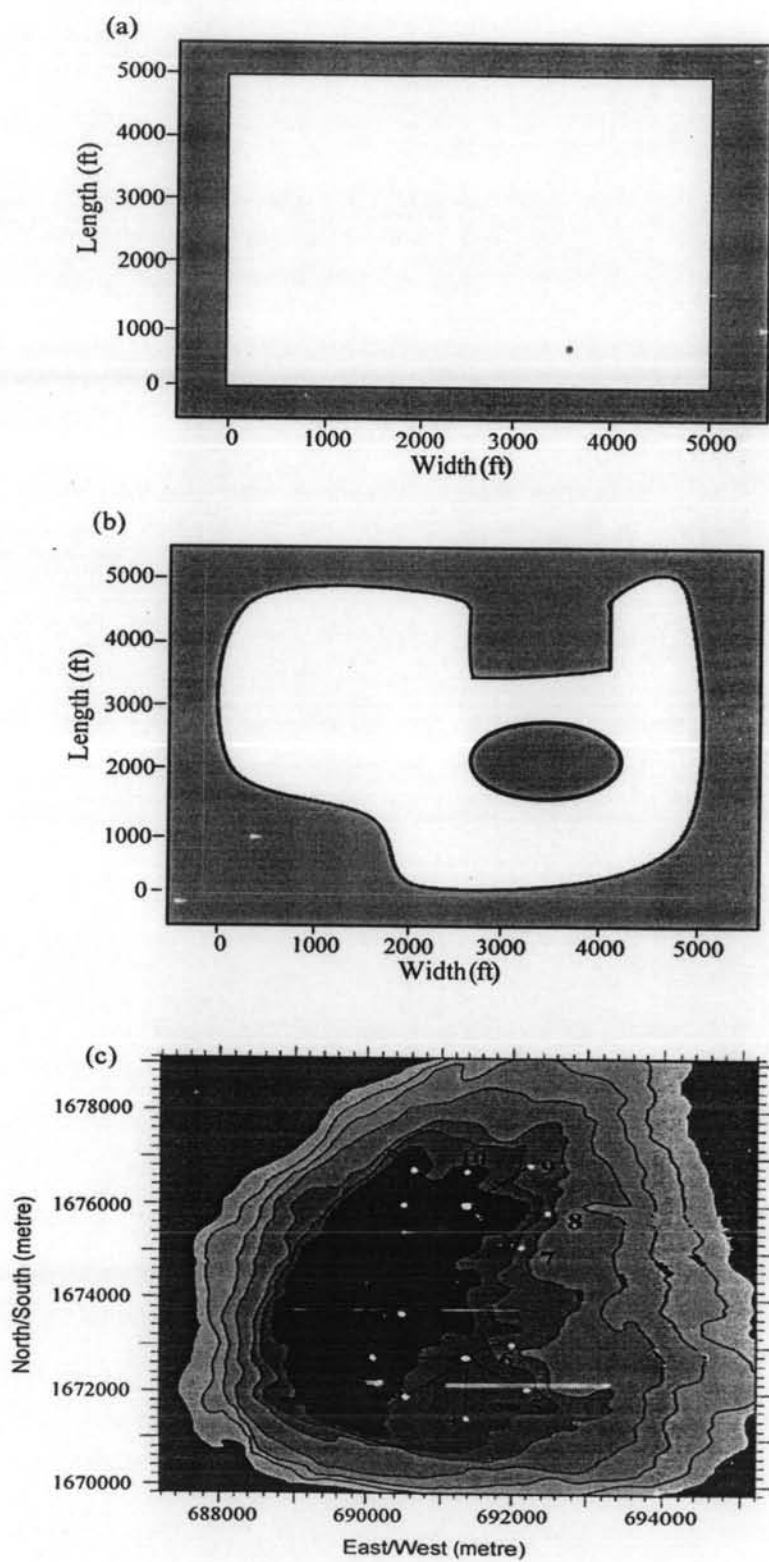


Figure 3.1 Geometries of modelling reservoir, (a) regular shape, (b) irregular shape, (c) carbonate reservoir.

3.2 Model Assumptions

In this work, some specifications of reservoir properties are assumed as follows otherwise stated:

1. The reservoir has a uniform thickness, h , which cancels throughout the equation.
2. The permeability, k , was assumed constant along the reservoir.
3. The gas (predominantly methane) behaves ideally, and so has a compressibility factor $Z = 1$.
4. The porosity and reservoir temperature are uniform throughout the reservoir.

3.3 Model Formulation

In the natural gas production, flow of natural gas into the well depends on the pressure drop in the reservoir, $p_r - p_w$, where p_r is average reservoir pressure and p_w is wellbore pressure. The relationship between flow rate and pressure drop occurring in the porous medium is very complex and depends on many parameters such as rock properties, fluid properties and flow regime.

For single phase flow in porous medium, the fluid velocity (\bar{V}) throughout the porous medium can be determined using the Darcy's law (Wilkes, 1999).

$$\bar{V} = -\frac{k}{\mu} \nabla p \quad (3-1)$$

where, k is the rock permeability, μ the gas viscosity, ∇p the pressure gradient.

The two dimensional mass balance equation (combining with Darcy's law) as a function of pressure in the rectangular coordinate can be written as (Wilkes, 1999),

$$\frac{\partial}{\partial x} \left(\frac{p}{ZT} \frac{hk}{\mu} \frac{\partial p}{\partial x} \right) + \frac{\partial}{\partial y} \left(\frac{p}{ZT} \frac{hk}{\mu} \frac{\partial p}{\partial y} \right) - \frac{MhR}{MW} = \varepsilon h \frac{\partial (p/ZT)}{\partial t} \quad (3-2)$$

where, ε is porosity; h , the reservoir thickness; M , the mass withdrawal rate per unit volume; MW , the molecular weight of gas; p , the reservoir pressure; R , the gas constant, T , the reservoir temperature; and Z , the compressibility factor.

The volumetric flow rate per volume (q_s) at standard conditions is given by,

$$q_s = \frac{M}{\rho_s} = \frac{MRT_s}{p_s MW} \quad (3-3)$$

Replacing q_s from above equation into Eq. (3-3) yields

$$\frac{\partial}{\partial x} \left(\frac{p}{ZT} \frac{hk}{\mu} \frac{\partial p}{\partial x} \right) + \frac{\partial}{\partial y} \left(\frac{p}{ZT} \frac{hk}{\mu} \frac{\partial p}{\partial y} \right) - \frac{q_s p_s h}{T_s} = \varepsilon h \frac{\partial (p/ZT)}{\partial t} \quad (3-4)$$

Defining the gas potential (compared with reference pressure, p_r) as

$$\phi = \int_{p_r}^p \frac{p}{Z\mu} dp \quad (3-5)$$

Assuming that reference pressure (p_r) is equal 0, Eq. (3-5) becomes

$$\phi = p^2/2\mu \quad (3-6)$$

or

$$p = (2\mu\phi)^{1/2} \quad (3-7)$$

Eq. (3-4) is rearranged to

$$\frac{\partial}{\partial x} hk \frac{\partial \phi}{\partial x} + \frac{\partial}{\partial y} hk \frac{\partial \phi}{\partial y} - \frac{q_s h T p_s}{T_s} = \varepsilon h \gamma \frac{\partial \phi}{\partial t} \quad (3-8)$$

$$\text{where, } \gamma = \frac{\mu}{p} = \frac{\mu}{\sqrt{2\mu\phi}}, \quad \beta = \varepsilon * \sqrt{\frac{\mu}{2}}$$

Using assumptions indicated previously, Eq. (3-8) for gas withdrawal from a reservoir becomes,

$$k\left(\frac{\partial^2 \phi}{\partial x^2} + \frac{\partial^2 \phi}{\partial y^2}\right) - \alpha q_s = \frac{\beta}{\sqrt{\phi}} \frac{\partial \phi}{\partial t} \quad (3-9)$$

where, $\alpha = \frac{Tp_s}{T_s}$

In case of gas injection into reservoir, the equation becomes

$$k\left(\frac{\partial^2 \phi}{\partial x^2} + \frac{\partial^2 \phi}{\partial y^2}\right) + \alpha q_s = \frac{\beta}{\sqrt{\phi}} \frac{\partial \phi}{\partial t} \quad (3-10)$$

In case of flow from the reservoir into the i^{th} well, (Figure 3.2 and Appendix A)

$$Q_i = \pm \frac{\pi h k (p_{wi}^2 - p_{bi}^2)}{\alpha \mu \ln \frac{r_e}{r_w} - 0.5} \quad (3-12)$$

where, plus and minus signs represent injection and withdrawal, respectively.

And the flow in the well (Appendix B),

$$Q_i = \pm \frac{\pi}{\sqrt{32}} \left(\frac{MW}{RT\rho_s} \right) \sqrt{\frac{\pm gD^5 (e^{\alpha_i L} p_i^2 - p_{wi}^2)}{f_i (e^{\alpha_i L} - 1)}} \quad (3-13)$$

where, $\alpha_i = 2MWg/RT$, plus and minus signs represent injection and withdrawal, respectively.

The volumetric flow rate per volume (q_s) is related to volume flow rate (Q_i) by

$$Q_i = q_s (\Delta x \Delta y h) \quad (3-14)$$

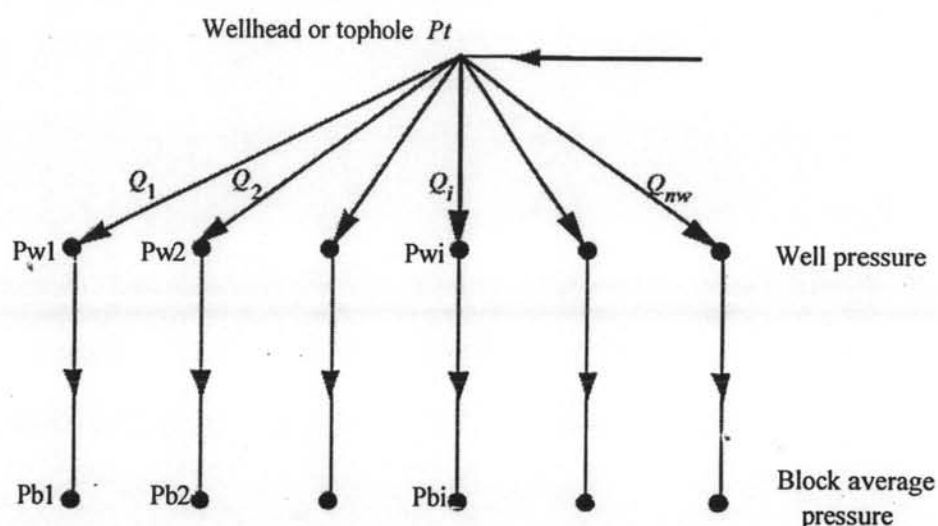


Figure 3.2 Flows in the block / well system (Wilkes, 1999).

3.4 Numerical Algorithm

In this section, numerical methods used to solve Eq. (3-9) were discussed in details which were finite difference and finite element methods. The finite difference method uses the alternating-direction implicit (ADI) scheme to discretize the governing equation. This is because the ADI scheme is a general method to solve the parabolic equation which is in the similar form of Eq. (3-9). It is coded using the FORTRAN programming language. For the finite element method, it is very sophisticated to code this method in the FORTRAN programming language. Consequently, the commercial finite element software package, FEMLAB, available in-house at the Petroleum and Petrochemical College, was chosen to solve the governing equation. The basic concepts of these algorithms are explained below.

3.4.1 Finite Difference Method

The ADI scheme provided by the finite difference methods was employed to discretize the governing equation into the same interval of time and space. It divides the geometrical shape by a number of rectangular blocks of uniform

dimensions, Δx and Δy , to represent the block area of petroleum reservoir. For example, the cross-sectional area of irregular reservoir is depicted in Figure 3.3. The black curves show the actual boundaries of the reservoir. Active blocks are represented by a number of rectangular blocks. Each block was assigned as a pair of subscript, (i, j) , in the x -, y - directions, respectively. Values of h (thickness), ε (porosity) and k (permeability) are associated with each block.

The reservoir was surrounded by inactive blocks and island at the center as shown by gray blocks, which represent impermeable rock or water, therefore no mass was transferred along these boundaries. Therefore, the ADI scheme does not apply in this area. The locations of active blocks taken into account in the simulation are shown in Table 3.1.

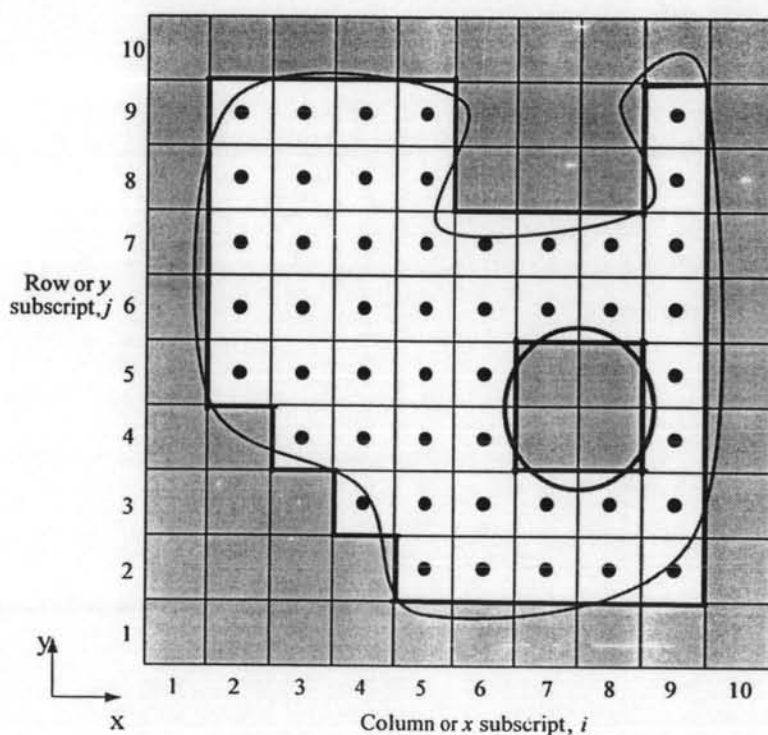


Figure 3.3 Subdivision of irregular reservoir into blocks (Wilkes, 1999).

Table 3.1 Active block indices

i	j	i	j	i	j	i	j
2	5	4	4	5	8	8	2
2	6	4	5	5	9	8	3
2	7	4	6	6	2	8	6
2	8	4	7	6	3	8	7
2	9	4	8	6	4	9	2
3	4	4	9	6	5	9	3
3	5	5	2	6	6	9	4
3	6	5	3	6	7	9	5
3	7	5	4	7	2	9	6
3	8	5	5	7	3	9	7
3	9	5	6	7	6	9	8
4	3	5	7	7	7	9	9

The ADI method can be applied into Eq. (3-9) at grid point (i, j) by divided the time

step, $\frac{\partial \phi}{\partial t}$, into two half time steps, i.e., $\frac{\phi_{i,j}^* - \phi_{i,j}^n}{\Delta t/2}$ and $\frac{\phi_{i,j}^{n+1} - \phi_{i,j}^*}{\Delta t/2}$.

From the governing equation,

$$k \left(\frac{\partial^2 \phi}{\partial x^2} + \frac{\partial^2 \phi}{\partial y^2} \right) - \alpha q_s = \frac{\beta}{\sqrt{\phi}} \frac{\partial \phi}{\partial t} \quad (3-9)$$

The first step, at the time step t^n to t^* , in the x-direction,

Eq. (3-9) becomes

$$k_{i,j} \delta_x^2 \phi_{i,j}^* + k_{i,j} \delta_y^2 \phi_{i,j}^n - (\alpha q_s)_{i,j} = \frac{\beta}{\sqrt{\phi_{i,j}^n}} \left(\frac{\phi_{i,j}^* - \phi_{i,j}^n}{\Delta t/2} \right) \quad (3-15)$$

Given the second order differential form, $\delta_x^2 \phi_{i,j}^*$ and $\delta_y^2 \phi_{i,j}^n$,

$$\delta_x^2 \phi_{i,j}^* = \frac{\phi_{i-1,j}^* - 2\phi_{i,j}^* + \phi_{i+1,j}^*}{\Delta x^2} \quad (3-16)$$

$$\delta_y^2 \phi_{i,j}^n = \frac{\phi_{i,j-1}^n - 2\phi_{i,j}^n + \phi_{i,j+1}^n}{\Delta y^2} \quad (3-17)$$

Eqs. (3-16) and (3-17) are placed into Eq. (3-15),

$$\begin{aligned} & (Cx)_{i,j} \sqrt{\phi_{i,j}^n} (\phi_{i-1,j}^* - 2\phi_{i,j}^* + \phi_{i+1,j}^*) + (Cy)_{i,j} \sqrt{\phi_{i,j}^n} (\phi_{i,j-1}^n - 2\phi_{i,j}^n + \phi_{i,j+1}^n) \\ & - \frac{\alpha \sqrt{\phi_{i,j}^n} (q_s)_{i,j} \Delta t}{2\beta} = \phi_{i,j}^* - \phi_{i,j}^n \end{aligned} \quad (3-18)$$

$$\text{where, } (Cx)_{i,j} = \frac{k_{i,j} \Delta t}{2\beta (\Delta x)^2}, \quad (Cy)_{i,j} = \frac{k_{i,j} \Delta t}{2\beta (\Delta y)^2}$$

Then, Eq. (3-15) becomes,

$$\begin{aligned} & -\lambda x_{i,j} \phi_{i-1,j}^* + (1 + 2\lambda x_{i,j}) \phi_{i,j}^* - \lambda x_{i,j} \phi_{i+1,j}^* = \lambda y_{i,j} \phi_{i,j-1}^n \\ & + (1 - 2\lambda y_{i,j}) \phi_{i,j}^n - \lambda y_{i,j} \phi_{i,j+1}^n - \delta_{i,j} \end{aligned} \quad (3-19)$$

$$\text{where, } \lambda x_{i,j} = (Cx)_{i,j} \sqrt{\phi_{i,j}^n}, \quad \lambda y_{i,j} = (Cy)_{i,j} \sqrt{\phi_{i,j}^n}, \quad \delta_{i,j} = \frac{\alpha \sqrt{\phi_{i,j}^n} (q_s)_{i,j} \Delta t}{2\beta}$$

The second step, at the time step t^* to t^{n+1} , in the y -direction

Eq. (3-9) becomes

$$k_{i,j} \delta_x^2 \phi_{i,j}^* + k_{i,j} \delta_y^2 \phi_{i,j}^{n+1} - (\alpha q_s)_{i,j} = \frac{\beta}{\sqrt{\phi_{i,j}^n}} \left(\frac{\phi_{i,j}^{n+1} - \phi_{i,j}^*}{\Delta t / 2} \right) \quad (3-20)$$

Eqs. (3-16) and (3-17) are placed into Eq. (3-20),

$$(Cy)_{i,j} \sqrt{\phi_{i,j}^n} (\phi_{i,j-1}^{n+1} - 2\phi_{i,j}^{n+1} + \phi_{i,j+1}^{n+1}) + (Cx)_{i,j} \sqrt{\phi_{i,j}^n} (\phi_{i,-1,j}^* - 2\phi_{i,j}^* + \phi_{i+1,j}^*) - \frac{\alpha \sqrt{\phi_{i,j}^n} (q_s)_{i,j} \Delta t}{2\beta} = \phi_{i,j}^{n+1} - \phi_{i,j}^* \quad (3-21)$$

$$\text{where, } (Cx)_{i,j} = \frac{k_{i,j} \Delta t}{2\beta (\Delta x)^2}, \quad (Cy)_{i,j} = \frac{k_{i,j} \Delta t}{2\beta (\Delta y)^2}$$

Then, the Eq. (3-20) becomes,

$$-\lambda y_{i,j} \phi_{i,j-1}^{n+1} + (1 + 2\lambda y_{i,j}) \phi_{i,j}^{n+1} - \lambda y_{i,j} \phi_{i,j+1}^{n+1} = \lambda x_{i,j} \phi_{i-1,j}^* + (1 - 2\lambda x_{i,j}) \phi_{i,j}^* - \lambda x_{i,j} \phi_{i+1,j}^* - \delta_{i,j} \quad (3-22)$$

$$\text{where, } \lambda x_{i,j} = (Cx)_{i,j} \sqrt{\phi_{i,j}^n}, \quad \lambda y_{i,j} = (Cy)_{i,j} \sqrt{\phi_{i,j}^n}, \quad \delta_{i,j} = \frac{\alpha \sqrt{\phi_{i,j}^n} (q_s)_{i,j} \Delta t}{2\beta}$$

The value of transmissibilities (λ) at the interface between blocks and reservoir boundaries must be zero, because the inactive block has zero permeability satisfying by the harmonic average in x- and y-directions as indicated in the following equations (Appendix C),

$$\lambda x_{i+1/2,j} = \frac{2\lambda x_{i,j} \lambda x_{i+1,j}}{(\lambda x_{i,j} + \lambda x_{i+1,j})} \quad (3-23)$$

$$\lambda y_{i,j+1/2} = \frac{2\lambda y_{i,j} \lambda y_{i,j+1}}{(\lambda y_{i,j} + \lambda y_{i,j+1})} \quad (3-24)$$

3.4.2 Finite Element Method

The FEMLAB software solves any combination of physical processes. The program is based on the finite element method. FEMLAB provides high speed, accuracy and varieties of postprocessing modes for multiphysics applications. The

modelling procedure involves the following steps, i.e., setting up the geometry, defining the subdomain and boundaries, creating a mesh, solving the model and postprocessing to investigate the results.

The governing equation in FEMLAB program can apply starting from Eq. (3-4) as shown,

$$\frac{\partial}{\partial x} \left(\frac{p}{T} \frac{k}{\mu} \frac{\partial p}{\partial x} \right) + \frac{\partial}{\partial y} \left(\frac{p}{T} \frac{k}{\mu} \frac{\partial p}{\partial y} \right) - \frac{q_s p_s}{T_s} = \varepsilon \frac{\partial (p/T)}{\partial t} \quad (3-25)$$

The steps in this method are described in Appendix F.